ChemComm

COMMUNICATION

View Article Online
View Journal | View Issue

Cite this: *Chem. Commun.*, 2024, **60**, 4326

Received 13th December 2023,
Accepted 13th March 2024

DOI: 10.1039/d3cc06088h

rsc.li/chemcomm

Ag–In–Zn–S alloyed nanocrystals as photocatalysts of controlled light-mediated radical polymerization†

Patrycja Kowalik,[ab] Piotr Bujak,* [a] Mateusz Penkala,[c] Anna Iuliano,[a] Ireneusz Wielgus,[a] Karolina Peret[a] and Adam Pron[a]

We report on the first case of the use of nonstoichiometric ternary (Ag–In–Zn–S) semiconductor nanocrystals as photoinitiators and photocatalysts of methyl methacrylate (MMA) polymerization. Two types of nanocrystals were tested, differing in their composition and characterized by red (λ_{max} = 731 nm) and green (λ_{max} = 528 nm) photoluminescence, respectively. Exploiting their reducing properties and capability of free radical generation we demonstrate that under ultraviolet (UV) radiation they effectively photoinitiate radical polymerization of MMA whereas under visible light (blue or green) they act as photocatalysts of living radical polymerization.

Light-mediated living radical polymerization can be achieved through one of the three possible strategies: (i) atom transfer radical polymerization (ATRP),[1] (ii) nitroxide-mediated radical polymerization (NMP)[2] and (iii) reversible addition fragmentation chain transfer polymerization (RAFT).[3] Metal complexes or small organic molecules are typically used as photocatalysts in these processes.[4] Narrow and wide band-gap semiconductor photocatalysts in their nanocrystalline form such as metal oxides: Bi_2O_3[5] and ZnO,[6] or metal chalcogenides *e.g.* CdSe,[7] or CdS,[8] as well as perovskite nanocrystals[9] and graphitic carbon nitride (g-C_3N_4)[10] are also tested. In the case of all these nanomaterials the term "photomediators" is frequently used which embraces both photoinitiators and photocatalysts.[11] Typical photoinitiators can efficiently initiate the polymerization process but are incapable of controlling the propagation and chain termination steps, at least to a significant extent. To the contrary, photocatalysts *via* their photocatalytic cycle may assure living character of the polymerization process.

Inorganic semiconductor nanocrystals tested to date such as ZnO or CdSe are characterized by relatively low-lying conduction bands (or in the molecular approach the LUMO levels) (Fig. 1). It should be noted that the data reported in Fig. 1 were determined for pH = 1.0 and for other values of pH they can differ by 0.2–0.3 eV at the most.[12] In any case, the electron transfer to typical vinyl monomers like MMA, showing a low value of the reduction potential (−1.86 V *vs.* NHE), is not possible.[8c] It was demonstrated, that in the case of CdS nanocrystals, in addition to electron transfer-driven initiation, it is possible to induce another type of the initiation process, namely *via* hole-transfer. This process leads to the oxidation of MMA, abstraction of a hydrogen atom form the methyl group and the formation of a stable acrylic-type radical.[8b] Photogeneration reactions supported by co-initiators *e.g.* 2-propanol[13] or water[14] are also known leading to intermediate radicals or to

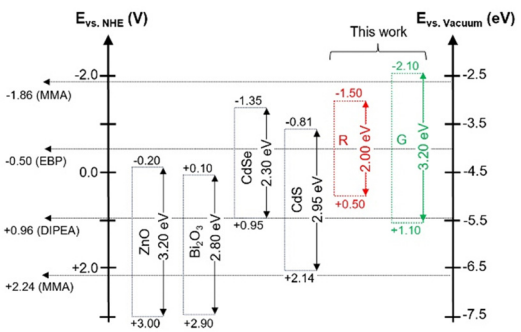

Fig. 1 Energy levels of selected binary (ZnO, Bi_2O_3, CdSe, CdS) and quaternary Ag–In–Zn–S (**R** and **G**) nanocrystals investigated in this research. The values are expressed on the absolute energy scale, *i.e.*, with respect to the vacuum level in eV (right). Their redox potentials *vs.* NHE electrode (in V) together with the corresponding redox potentials of MMA, ethyl α-bromophenylacetate (EBP) and *N*,*N*-diisopropylethylamine (DIPEA) (left).

[a] *Warsaw University of Technology, Faculty of Chemistry, Noakowskiego 3, Warsaw 00-664, Poland. E-mail: piotrbujakchem@poczta.onet.pl*
[b] *Institute of Physical Chemistry, Polish Academy of Science, Kasprzaka 44/52, Warsaw 01-224, Poland*
[c] *Institute of Chemistry, Faculty of Science and Technology, University of Silesia, Szkolna 9, Katowice 40-007, Poland*

† Electronic supplementary information (ESI) available: Experimental sections, characterization methods, EDS, HR-TEM and XRD patterns of alloyed Ag-In-Zn-S nanocrystals, ^{1}H and ^{13}C NMR spectra of the reaction mixture, SEC profiles of PMMA. See DOI: https://doi.org/10.1039/d3cc06088h

radical cations if tertiary amines are used.[8c] In yet another approach nanocrystals are capped with special ligands capable of generating radicals.[15] Large majority of the above mentioned papers describe nanocrystalline materials which can be considered as photoinitiators or photomediators but in strict terms they cannot be regarded as photocatalysts.

There exist however reports on semiconductor nanocrystals exhibiting typical features of photocatalysts. Egap *et al.*[7] prepared colloidal CdSe nanocrystals (3.3 nm in size) characterized by a relatively high value of their reduction potential (−1.35 V *vs.* NHE) and a relatively low value of the oxidation potential (+ 0.95 V *vs.* NHE). They were tested as catalysts in the ATRP process of acrylates in the presence of ethyl α-bromophenylacetate (EBP) and *N*,*N*-diisopropylethylamine (DIPEA). Appropriate tuning of the valence and conduction bands positions (or HOMO and LUMO levels in the molecular approach) with respect to the energy of the used blue light (480 nm) promoted: (i) reduction of EBP to $EBP^{\bullet -}$ (−0.5 V *vs.* NHE)[16] and (ii) oxidation of DIPEA to $DIPEA^{\bullet +}$ (+ 0.96 V *vs.* NHE),[17] the latter process supplying electrons for the reduction reaction and closing the photocatalytic cycle.

In one of our recent papers we reported a new method of the preparation of ternary Ag–In–Zn–S nanocrystals involving indium(II) chloride (In_2Cl_4) as a new indium precursor together with $AgNO_3$ and zinc stearate as precursors of silver and zinc. This new procedure allowed for the preparation of nanocrystals whose emission spectra could be controllably tuned in the spectral range from 530 to 730 nm.[18] Two types of Ag–In–Zn–S nanocrystals, distinctly differing in their composition and emitting red (λ_{max} = 731 nm, termed (**R**)) and green (λ_{max} = 528 nm, termed (**G**)) light, respectively, were tested as photocatalysts in the reactions of aromatic aldehydes reduction.[19] In principle, taking into account their photophysical and redox properties, the same nanocrystals should be considered as promising candidates for new type of photoinitiators and photocatalysts in different types of ATRP processes. In the investigations aimed at the elaboration of new photocatalysts of controlled radical polymerization two types of nanocrystals differing in compositions tested, namely $Ag_{1.0}In_{1.5}Zn_{0.3}S_{3.3}$ (**R**) and $Ag_{1.0}In_{10.3}Zn_{12.4}S_{11.8}$ (**G**). **R** nanocrystals were spherical in shape (diameter, $D = 6.2 \pm 1.1$ nm) whereas **G** ones exhibited rod-like morphology (length, $L = 9.9 \pm 2.2$ nm and diameter $D = 3.1 \pm 0.7$ nm). By X-ray they exhibited alloyed-type structure being intermediated between the structures of orthorhombic $AgInS_2$ (JCPDS 00-025-1328) and wurtzite ZnS (JCPDS 00-036-1450). Their energy-dispersive spectra (EDS), HR-TEM images and powder diffractograms can be found in Fig. S1–S3 of ESI.† The main advantage of these nonstoichiometric nanocrystals, unobtainable in the case of previously investigated binary nanocrystals *e.g.* CdSe, is the possibility of precise tuning of their band gap and, in consequence, their redox properties. The band gaps energies determined for **R** and **G** were equal to E_g = 2.0 eV and E_g = 3.2 eV, respectively. Similarly their reduction potentials significantly differed, corresponding to −1.5 V for **R** nanocrystals and to −2.1 V (*vs.* NHE) for **G** ones.[19] These are much higher values as compared to those reported for nanocrystals of CdSe and other binary semiconductors (see Fig. 1). Reduction potentials of both (**R** and **G**) types of nanocrystals fall in the range of the corresponding potentials of typical ATRP initiators and are close to that determined for MMA (−1.86 V *vs.* NHE).

Moreover detailed spectroscopic investigations revealed unusually long average emission lifetimes of 1.50 and 0.80 μs, for **R** and **G** nanocrystals, respectively.[19]

Photopolymerizations of MMA were carried out in standard conditions using a THALESNano photoreactor in which LED-originating, monochromatic radiation of different wavelengths could be selected (Fig. 2a). In all tests the same volume of the colloidal dispersions of nanocrystals in C_6D_6 (0.1 mL) was used, which corresponds to 1.3×10^{-3} mmol and 1.5×10^{-4} mmol of silver content in **R** and **G** nanocrystals, respectively. Two types of polymerizations were carried out: (i) bulk polymerizations (6 hours; 8 mL MMA) and (ii) polymerizations in benzene-d_6 (6 hours; 8 mL MMA; MMA/solvent = 1/1 v/v). The use of the deuterated solvent enabled us to perform direct analytical (NMR) tests of the reaction mixtures. The results of the test polymerizations are presented in Table S1 (ESI†) whereas all registered ^1H and ^{13}C NMR are collected in Fig. S4–S8 of ESI.†

Tests of bulk photopolymerizations of MMA in the presence of **R** and **G** nanocrystals were performed using monochromatic light of three different wavelengths: 356 nm (UV); 457 nm (blue) and 523 nm (green). Absorption, excitation and emission spectra of the used nanocrystals dispersions are comparatively

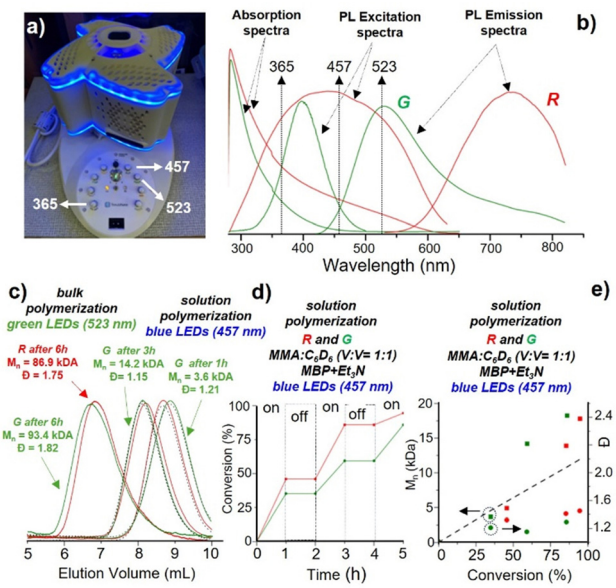

Fig. 2 (a) Photograph of the experimental setup – photoreactor; (b) absorption, photoluminescence excitation and emission spectra of toluene dispersions of **R** and **G** nanocrystals; (c) SEC profiles of PMMA prepared in bulk and solution ("on/off" experiment) polymerization; (d) plot of monomer conversion *versus* time of polymerization in the presence "on" and in the absence "off" of blue (457 nm) light; (e) plot of M_n (squares) and *Đ* (circles) *versus* conversion of monomer in the presence of blue (457) light (the black dash line indicates the theoretical M_n in an ideal living polymerization). MMA : Et_3N : MBP = 125.0 : 1.6 : 1.0, introducing additionally C_6D_6 as a solvent (*v*/*v* = 1/1).

presented in Fig. 2b. Bulk photopolymerizations in the presence of UV radiation yielded very similar conversions of MMA to PMMA, independently of the nanocrystals used, *i.e.* 24% and 25% for **R** and **G** photoinitiators, respectively.

As determined by Size Exclusion Chromatography (SEC), the resulting polymers exhibited high molecular masses (M_n) and large molecular weight distribution ($Đ$): M_n = 313.8 kDa, $Đ$ = 2.53 (**R**); M_n = 134.9 kDa $Đ$ = 3.07 (**G**) (for details see Fig. S9a and b of ESI†). With blue light only **R** nanocrystals initiated the photopolymerization, albeit the conversion was rather low (14.5%). In the presence of green light both (**R** and **G**) nanocrystals turned out to be inactive and no PMMA was formed. Photopolymerization under UV radiation is initiated by surfacial nanocrystals ligands (R–(C═O)SH) which are being photochemically converted into –(C═O)S$^{\bullet}$ radicals, as proven by EPR investigations.[19] Thus, the UV photoinitiation inevitably leads to a decrease of the population of the surfacial ligands and, by consequence, lowering of the colloidal stability of nanocrystals. Moreover, this process is totally uncontrollable, resulting in large values of $Đ$. In the presence of green light both (**R** and **G**) nanocrystals turned out to be inactive and no PMMA was formed. It should be noted that radicals are generated even under green light, as evidenced by EPR spectra of the products of their trapping with DMPO (see Fig. S10 of ESI†) but in these conditions they are unable to initiate the polymerization of MMA.

Considering all outlined above disadvantages of the UV photoinitiation we decided to limit our research to photopolymerization under blue and green light. The photopolymerization conditions were modified by addition of triethylamine (Et_3N), an electron donor at a molar ratio MMA : Et_3N = 75 : 1 or methyl α-bromophenylacetate (MBP), an ATRP initiator at higher MMA : MBP molar ratio of 125. Photopolymerizations carried out in the presence of Et_3N and under blue light resulted in conversions of 41.3% and 13.8%, for nanocrystals **R** and **G**, respectively. In the former case, the obtained PMMA exhibited a high molecular mass of M_n = 318.7 kDa, together with large $Đ$ = 2.9 (for details see Fig. S9c of ESI†). Low conversions were obtained under green light: 15.0% for MMA/Et_3N/**R** and inferior to 10% in the case of MMA/MBP/**R**. No polymerization products were detected neither for MMA/Et_3N/**G** and MMA/MBP/**G** under green light initiation. Successful polymerizations under green light were however achieved for mixtures consisting of MMA : Et_3N : MBP in the molar ratio 125.0 : 1.6 : 1.0. **R** nanocrystals yielded PMMA characterized by M_n = 86.9 kDa and $Đ$ = 1.75 with 98% conversion. Lower conversion was determined in the case of **G** nanocrystals (63%) and the resulting polymer exhibited M_n = 93.4 kDa and $Đ$ = 1.82 (Fig. 2c). These experiments clearly corroborate the formation of a catalytic cycle typical of ATRP. Lower conversions measured for **G** photocatalysts, as compared to **R** ones, have their origin in reduced absorption of green light by these nanocrystals (Fig. 2b), which effectively eliminates uncontrolled photoinitiation but at the same time lowers their photocatalytic activity. In order to more precisely elucidate the controlled nature of the photopolymerization in the presence of nanocrystals we performed this process for the mixture MMA : Et_3N : MBP = 125.0 : 1.6 : 1.0, introducing additionally C_6D_6 as a solvent (v/v = 1/1). The polymerizations were carried out under blue light in intervals "on/off" consisting of one hour of exposure to light followed by one hour with light switched off (Fig. 2d). In the case of **R** nanocrystals, after the first hour of exposure M_n of the formed polymer reached 4.9 kDa ($Đ$ = 1.32), being almost tripled after the no exposure period, followed by the second hour of exposure (M_n = 13.9 kDa, $Đ$ = 1.41). The same trend was observed for **G** nanocrystalline photocatalysts (M_n = 3.6 kDa, $Đ$ = 1.21) after the first exposure cycle and 14.2 kDa, $Đ$ = 1.15 after the second one. Summarizing, after the full 5 hours cycle (three hours of exposure and two intervals with the light switched off) high conversions were reached (94.5% for **R** and 85.9 for **G**) with M_n steadily increasing and $Đ$ remaining low and relatively unchanged (Fig. 2e), all in accordance with the ATRP mechanism. However, the measured M_n values are close to the theoretically predicted for living polymerization up to 50% conversion only. For higher conversion deviations from linearity are observed. This means that the proposed new photocatalytic system requires further optimization in terms of the monomer concentration and the reagents molar ratios. For the final samples (3 hours of exposure + two no exposure intervals, either **R** or **G** photocatalysts) MS MALDI_TOF measurements were performed (Fig. S11 for **R** nanocrystals and Fig. S12 for **G** ones, ESI†). Two sets of peaks can be distinguished in their spectra (Fig. 3a). The group of more intensive peaks can be ascribed to molecular peaks $[M_1 + K]^+$ of macromolecules terminated on one end with the MBP initiator fragment and with hydrogen on the other. The second set of

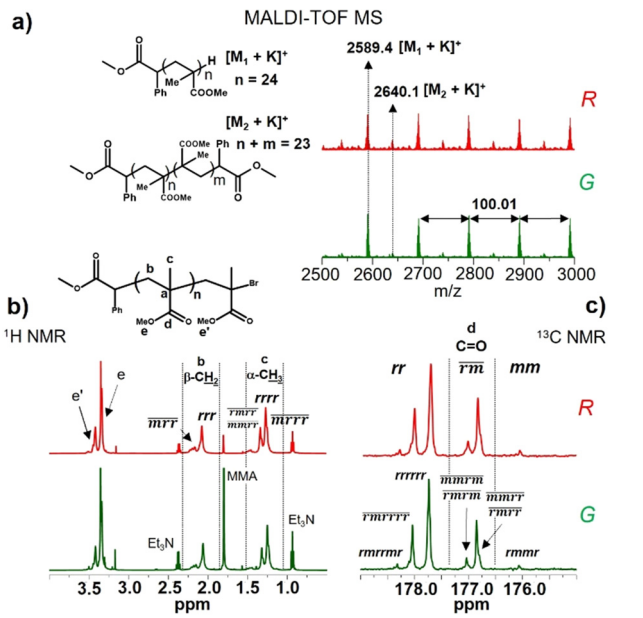

Fig. 3 (a) MALDI-TOF spectra of PMMA synthesized in the presence of **R** and **G** nanocrystals as photocatalysts; reaction mixture MMA : Et_3N : MBP = 125.0 : 1.6 : 1.0 dissolved in C_6D_6 (v/v = 1/1) (b) ^{1}H and (c) ^{13}C NMR spectra (in benzene-d_6) of the same reaction mixture with **R** and **G** nanocrystals as photocatalysts.

less intensive molecular peaks $[M_2 + K]^+$ corresponds to chains terminated with the initiator (MBP) fragments at both ends. In both sets individual peaks are uniformly separated by m/z = 100, which strictly corresponds to one mer of PMMA. Microstructures of these chains were investigated by ^{1}H and ^{13}C NMR. In the registered ^{1}H NMR spectra (Fig. 3b) signals splittings are observed in the spectral ranges 1.15–1.50 ppm (α-CH_3) and 3.33–3.41 ppm (CH_3O) corresponding to odd sequences *i.e.* configurational triads and pentads whereas in the range 2.00-2.25 ppm (β-CH_2) even sequences, namely configurational tetrads, can be distinguished.[20] A distinct signal at 3.52 ppm originates from the alkoxy (CH_3O) substituents in terminal MMA group containing bromine, in accordance with the ATRP mechanism.[21] Consistently, in the aliphatic part of the corresponding ^{13}C NMR spectrum (Fig. S7, ESI†) lines ascribed to odd sequences (configurational triads) can be distinguished at 17.5–19.7 ppm (α-CH_3) and 45.2–45.4 ppm (α-C) as well as signals originating from even sequences (tetrads) in the spectral range of 54–56 ppm (β-CH_2).[22] Overlapping signals at 51.4–51.6 ppm should be attributed to the presence of CH_3O groups whereas a clear signal at 31.2 ppm should be considered as originating from the CH unit in the chain end group as derived from the analysis of the MALD-TOF spectra. This attribution is additionally corroborated by the ^{13}C NMR spectra recorded at different stages of the MBP-initiated polymerization of MMA as well as by previously reported literature data.[23] In the case of the signals ascribed to the carbonyl groups in PMMA located in the spectral range from 175 to 179 ppm (Fig. 3c) the observed splittings allow to distinguish longer configurational sequences such as pentads and heptads.[24] Quantitative analyses of the ^{1}H and ^{13}C NMR spectra registered for PMMA obtained with the **R** and **G** photocatalysts reveal the chain microstructure typical of radical polymerization. In particular, it is characterized by strong domination of syndiotactic sequences *i.e. rr* triads (∼ 70%) with significantly smaller contribution of *rm* triads (∼30%) and *mm* triads content falling below 1%.

To unequivocally confirm the photocatalytic activity of Ag–In–Zn–S nanocrystals in controlled radical polymerizations, RAFT bulk polymerizations of MMA were performed under blue light, in the presence of **R** nanocrystals. In all cases PMMA was obtained with conversions reaching 95% (see ^{1}H NMR and MALDI-TOF spectra presented in ESI†).

To summarize, toxic metals-free, nonstoichiometric quaternary Ag–In–Zn–S, unlike previously studied binary stoichiometric semiconductor nanocrystals, exhibit tunable, composition dependent redox properties. Appropriate tuning of their reduction potential, combined with their capability of free radicals generation, allows for their use as photoinitiators of radical polymerization under UV-radiation. Under visible light (either blue or green) the above mentioned uncontrollable photoinitiation is drastically reduced and the ternary nanocrystals can be used as photocatalysts for visible-light-mediated living radical polymerization using the ATRP approach. In these conditions nanocrystals assure controlled reduction of MBP and oxidation of amine (electron donor), resulting in strict control of M_n which increases with the polymerization time while the $Đ$ index remains low.

This work was supported by the National Science Centre of Poland, Grant No. 2022/45/B/ST5/02120. The research was carried out on devices purchased with funds provided by the Warsaw University of Technology within the Excellence Initiative: Research University (IDUB) programme. P. K. wish to acknowledge financial support from the Foundation for Polish Science (FNP) in a form of START fellowship.

Conflicts of interest

There are no conflicts to declare.

Notes and references

1 (*a*) B. P. Fors and C. J. Hawker, *Angew. Chem., Int. Ed.*, 2012, **51**, 8850; (*b*) X. Pan, M. A. Tasdelen, J. Laun, T. Junkers, Y. Yagci and K. Matyjaszewski, *Prog. Polym. Sci.*, 2016, **62**, 73.
2 Y. Guillaneuf, D. Bertin, D. Gigmes, D.-L. Versace, J. Lalevée and J.-P. Fouassier, *Macromolecules*, 2010, **43**, 2204.
3 (*a*) J. Xu, K. Jung, A. Atme, S. Shanmugam and C. Boyer, *J. Am. Chem. Soc.*, 2014, **136**, 5508; (*b*) Y. Zhao, Y. Chen, H. Zhou, Y. Zhou, K. Chen, Y. Gu and M. Chen, *Nat. Synth.*, 2023, **2**, 653; (*c*) C. Zhou, Z. Zhang, W. Li and M. Chen, *Angew. Chem., Int. Ed.*, 2024, **63**, e202314483.
4 C. Wu, N. Corrigan, C.-H. Lim, W. Liu, G. Miyake and C. Boyer, *Chem. Rev.*, 2022, **122**, 5476.
5 K. Hakobyan, T. Gegenhuber, C. S. P. McErlean and M. Müllner, *Angew. Chem., Int. Ed.*, 2019, **58**, 1828.
6 Z. Y. Huang, T. Barber, G. Mills and M. B. Morris, *J. Phys. Chem.*, 1994, **98**, 12746.
7 Y. Huang, Y. Zhu and E. Egap, *ACS Macro Lett.*, 2018, **7**, 184.
8 (*a*) A. J. Hoffman, G. Mills, H. Yee and M. R. Hoffmann, *J. Phys. Chem.*, 1992, **96**, 5546; (*b*) L. Katsikas, J. S. Veličković, H. Weller and I. G. Popović, *J. Therm. Anal.*, 1997, **49**, 317; (*c*) N. C. Strandwitz, A. Khan, S. W. Boettcher, A. A. Mikhailovsky, C. J. Hawker, T.-Q. Nguyen and G. D. Stucky, *J. Am. Chem. Soc.*, 2008, **130**, 8280.
9 Y. Zhu, Y. Liu, K. A. Miller, H. Zhu and E. Egap, *ACS Macro Lett.*, 2020, **9**, 725.
10 Q. Fu, Q. Ruan, T. G. McKenzie, A. Reyhani, J. Tang and G. G. Qiao, *Macromolecules*, 2017, **50**, 7509.
11 Y. Zhu and E. Egap, *ACS Polym. Au*, 2021, **1**, 76.
12 A. J. Nozik, *Ann. Rev. Phys. Chem.*, 1978, **29**, 189.
13 A. L. Stroyuk, V. M. Granchak and S. Y. Kuchmii, *Theor. Exp. Chem.*, 2001, **37**, 350.
14 S. Dadashi-Silab, A. M. Asiri, S. B. Khan, K. A. Alamry and Y. Yagci, *J. Polym. Sci., Part A: Polym. Chem.*, 2014, **52**, 1500.
15 Y.-C. Wong, J. De Andrew Ng and Z.-K. Tan, *Adv. Mater.*, 2018, **30**, 1800774.
16 J. C. Theriot, C.-H. Lim, H. Yang, M. D. Ryan, C. B. Musgrave and G. M. Miyake, *Science*, 2016, **352**, 1082.
17 J. Scharz and B. Köning, *Green Chem.*, 2016, **18**, 4743.
18 P. Kowalik, P. Bujak, M. Penkala, A. M. Maroń, A. Ostrowski, A. Kmita, M. Gajewska, W. Lisowski, J. W. Sobczak and A. Pron, *Chem. Mater.*, 2022, **34**, 809.
19 P. Kowalik, P. Bujak, M. Penkala, W. Tomaszewski, W. Lisowski, J. W. Sobczak, D. Siepietowska, A. M. Maroń, J. Polak, M. Bartoszek and A. Pron, *Chem. Mater.*, 2023, **35**, 6447.
20 H. L. Frisch, C. L. Mallows, F. Heatley and F. A. Bovey, *Macromolecules*, 1968, **1**, 533.
21 T. Nishikawa, M. Kamigaito and M. Sawamoto, *Macromolecules*, 1999, **32**, 2204.
22 Y. Inoue, A. Nishioka and R. Chûjô, *Polym. J.*, 1971, **2**, 535.
23 H. Janeczek, Z. Jedlinski and I. Bosek, *Macromolecules*, 1999, **32**, 4503.
24 P. Bujak, M. Matlengiewicz, M. Pasich and N. Henzel, *Polym. Bull.*, 2010, **64**, 259.